United Kingdom Atomic Energy Authority

UKAEA FUS 556

K.G. McClements, R.J. McKay

The orbital dynamics and collisional transport of trace massive impurity ions in rotating plasmas

The orbital dynamics and collisional transport of trace massive impurity ions in rotating plasmas

K.G. McClements, R.J. McKay

EURATOM/UKAEA Fusion Association, Culham Science Centre, OX14 3DB, Abingdon, UK

UKAEA FUS 556

EURATOM/UKAEA Fusion

The orbital dynamics and collisional transport of trace massive impurity ions in rotating plasmas

KG McClements, RJ McKay

August 2009

EURATOM/UKAEA Fusion Association
Culham Science Centre
Abingdon
Oxfordshire
OX14 3DB
United Kingdom

Telephone: +44 1235 466303
Fax: +44 1235 466435

The orbital dynamics and collisional transport of trace massive impurity ions in rotating tokamaks

K. G. McClements,[1] & R. J. McKay[2]

[1] *EURATOM/UKAEA Fusion Association, Culham Science Centre, Abingdon, Oxfordshire, OX14 3DB, United Kingdom*

[2] *University of Glasgow, Department of Physics and Astronomy, Glasgow, G12 8QQ, UK*

Abstract

Massive impurity ions in rotating tokamak plasmas have mean toroidal velocities that can greatly exceed the thermal speed of those ions. The effects of this hypersonic rotation on particle orbits and collisional transport are explored in the trace limit by considering the role of centrifugal and Coriolis forces in a co-rotating frame. Impurity ions of sufficiently high mass are deeply trapped by a centrifugal potential well in the outer plasma midplane, with a bounce period that is shorter than both the bounce period of magnetically-trapped ions and the collision time. The collisional diffusivity in this regime is shown to be higher than that of a non-rotating plasma. Irrespective of the collisionality regime, it is demonstrated that the interaction of massive impurity ions with bulk ions leads to an outward advection that is proportional to the impurity ion mass and can exceed the pinch velocity associated with the loop voltage. Due to modifications to the effective magnetic field arising from the Coriolis force, the increase in transport is greatest for relatively low charge states of massive impurity ions in plasmas rotating in the same direction as the plasma current. These effects are quantified analytically and using test-particle simulations of tungsten (W) and molybdenum (Mo) transport in transonically-rotating spherical tokamak plasmas. It is shown that the collisional confinement time of W ions in such plasmas can be two orders of magnitude shorter than the confinement time in the absence of rotation.

1. Introduction

Tokamak plasmas always contain ions of species other than the dominant fuel species, due to the sputtering of material from plasma-facing solid surfaces or fusion reactions. The presence of such impurity ions is generally undesirable, since it degrades the fusion fuel and enhances radiative energy losses from the plasma. Experimental and theoretical studies of impurity transport thus play an important role in the prediction of overall plasma performance in future devices. Tungsten (W) is an impurity species that is of particular relevance in this respect: it is currently the material of choice for the divertor in the burning plasma ITER device [1], and also a proposed spherical tokamak Component Test Facility (CTF) [2], due to its high melting point and the fact that tritium co-deposition is an unavoidable consequence of using carbon as a divertor material. Bulk W and W-coated tiles will be included in a new first wall that will be installed in the JET tokamak during an extended shutdown in 2009-2010 [3], and over the past few years progressively greater quantities of W have been incorporated into the first wall of the Asdex Upgrade tokamak [4]. It is therefore timely to re-examine theoretically the behaviour of heavy impurity ions, in particular tungsten ions, under tokamak conditions.

Compared to other impurity species typically found in tokamak plasmas, W ions have very high mass ($A = 184$ in the case of the most common isotope) and, in present-day devices, tend to be incompletely ionized: the last ionization potential of a species with nuclear charge Ze (e being the proton charge) is approximately equal to $Z^2 \times 13.6\,\mathrm{eV}$, which in the case of W ($Z = 74$) is more than an order of magnitude higher than typical tokamak temperatures. Tungsten ions in tokamaks thus tend to have a relatively low charge-to-mass ratio, and a thermal speed that is much lower than that of the bulk ions. An important consequence of the latter property is that in the presence of toroidal rotation velocities that are comparable to (or a significant fraction of) the bulk ion thermal speed, W ions will be dragged collisionally by the bulk ions at a rotation velocity v_φ that is hypersonic in terms of their own thermal speed v_Z, i.e. $v_\varphi \gg v_Z$, irrespective of their velocity distribution when they first enter the plasma. In these circumstances centrifugal and Coriolis forces play a key role in the collisional dynamics of the ions. For example, as we will discuss in the next section, particle trapping in the hypersonic regime is caused mainly by the centrifugal force rather than the magnetic mirror force.

Our aim in the present paper is to determine the orbits of heavy trace impurity ions in the hypersonic regime, and to explore the consequences of these orbits for collisional transport. A similar approach to the modelling of impurity transport in rotating tokamaks was adopted by Wong and Cheng [5], prompted by measurements of impurity radiation from the PLT [6] and TFTR [7] tokamaks. We extend the work of Wong and Cheng by obtaining analytical expressions for the bounce frequency of centrifugally-trapped heavy ions (section 2) and the collisional transport coefficients of such ions (section 3). In section 4 we use results from a test-particle simulation code to compare the collisional confinement times of heavy impurity ions in stationary and transonically-rotating spherical tokamak plasmas. In section 5 we summarise our results and briefly consider their significance in the context of past, present and future tokamaks containing tungsten impurity ions.

2. Centrifugal trapping

By considering force balance in the absence of dissipation within a single flux surface of a toroidally-rotating hydrogenic plasma, Wesson [8] showed that the density distribution of trace impurity ions on that surface is given by

$$n_Z = n_{Z0} \exp\left[\left(1 - \frac{T_e}{T_i + T_e} Z \frac{m_i}{m_Z}\right) \frac{m_Z \Omega_\varphi^2 R^2}{2T_Z}\right], \tag{1}$$

where n_{Z0} is a constant for the flux surface, T_e, T_i and T_Z denote electron, bulk ion and impurity ion temperatures, m_i and m_Z denote bulk ion and impurity ion mass, Z is the impurity ion charge state, Ω_φ is the toroidal rotation frequency of the plasma on a flux surface (assumed to be rotating as a rigid body), and R is major radial distance. Equation (1) is valid if T_e, T_i and T_Z as well as Ω_φ are constant on the flux surface. Impurity ions in tokamaks are strongly coupled via collisions to bulk ions, thereby ensuring that $T_Z \simeq T_i$ [9]. For an incompletely ionized species such as W, the value of the exponent in equation (1) is reduced only slightly by the Z-dependent term in the brackets, which arises from the presence of an electric field within the flux surface. It is thus clear that in the hypersonic regime ($\Omega_\varphi^2 R^2 \gg T_Z/m_Z$) impurity ions will be strongly concentrated in the outer plasma midplane. This result was in fact first demonstrated numerically (for Ar^{18+} ions) by Wong [10] several years before Wesson's analytical treatment [8].

We now consider the implications of this result for collisionless particle orbits. The fact that impurity ions are restricted to a region close to the outer midplane indicates that they are trapped poloidally, primarily by a centrifugal potential well rather than the magnetic field. To quantify the trapping effect of the centrifugal potential we first note that, in the absence of collisions, the impurity ion equation of motion in a frame rotating toroidally at frequency Ω can be written in the form [5]

$$m_Z \frac{d\mathbf{v}}{dt} = Ze\left(\mathbf{E} + \mathbf{v} \times \mathbf{B}\right) + \frac{1}{2} m_Z \Omega^2 \nabla(R^2) + 2m_Z \Omega \mathbf{v} \times \hat{\mathbf{e}}_Z, \tag{2}$$

where $\mathbf{E}$ and $\mathbf{B}$ denote the electric and magnetic fields in the rotating frame and $\hat{\mathbf{e}}_Z$ is the unit vector in the vertical direction (i.e. the direction of the rotation axis). Equation (2) can be obtained by writing down the standard Lagrangian of a nonrelativistic charged particle in an electromagnetic field in terms of inertial frame coordinates [11], making the coordinate transformation $\varphi' = \varphi - \Omega t$ where φ is toroidal angle, and then determining the corresponding Euler-Lagrange equations. The two last terms on the right hand side of equation (2) represent the centrifugal and Coriolis forces on the ion. It is apparent from equation (2) that the latter in effect introduces a vertical magnetic field to the equilibrium, the total effective field being

$$\mathbf{B}_* \equiv \mathbf{B} + \frac{2m_Z}{Ze} \Omega \hat{\mathbf{e}}_Z. \tag{3}$$

If $\mathbf{B}_*$ rather than $\mathbf{B}$ is taken to be the magnetic field, there is no Coriolis force as such and hence no Coriolis drift [12]. In the nonrelativistic limit $\mathbf{B}$ itself is unaffected by the transformation from the laboratory to the rotating frame, while $\mathbf{E}$ is related to the electric field in the laboratory frame $\mathbf{E}_i$ by the expression

$$\mathbf{E} = \mathbf{E}_i + \Omega \nabla \Psi, \tag{4}$$

where Ψ is the poloidal flux, defined such that the equilibrium magnetic field is given by $\mathbf{B} = RB_\varphi \nabla \varphi + \nabla \Psi \times \nabla \varphi$ where B_φ is the toroidal magnetic field. With this convention, the plasma current is oriented in the negative φ direction if Ψ increases from the magnetic axis to the plasma edge, in which case $\Omega < 0$ for a frame rotating in the co-current direction. In the limit of ideal magnetohydrodynamics (MHD), the laboratory frame electric field is simply equal to $-\Omega_\varphi \nabla \Psi$ [13]. By transforming to a frame rotating at frequency $\Omega = \Omega_\varphi$ we thus eliminate the ideal MHD part of the electric field. However, there remains a nonvanishing field in this frame, arising from the requirement of quasineutrality in a rotating plasma containing only trace quantities of impurity ions [14]:

$$\mathbf{E} = -\frac{m_i}{2e} \nabla \left(\frac{T_e \Omega_\varphi^2 R^2}{T_i + T_e} \right). \tag{5}$$

Substituting this expression into equation (2), taking the scalar product with $\mathbf{v}$, assuming that $T_e \Omega_\varphi^2/(T_e + T_i)$ does not vary significantly along the particle trajectory, and identifying the local rotation rate of the plasma with that of the frame (i.e. setting $\Omega_\varphi = \Omega$), we deduce the existence of an energy invariant

$$\mathcal{E} \equiv \frac{1}{2} m_Z \left[v^2 - \Omega^2 R^2 \left(1 - \frac{Z m_i T_e}{m_Z (T_i + T_e)} \right) \right], \tag{6}$$

in addition to the toroidal canonical momentum invariant

$$P_\varphi = m_Z R (v_\varphi + \Omega R) + Ze\Psi, \tag{7}$$

where v_φ is the toroidal velocity component in the rotating frame. For thermalised impurity ions the magnetic moment $\mu = m_Z v_\perp^2/(2B_*)$, where $v_\perp$ is velocity perpendicular to the effective magnetic field $\mathbf{B}_*$, is also approximately conserved in the rotating frame, as it is in the laboratory frame, but it should be noted that the effective field direction differs in the two frames. For low ionization states of a heavy impurity species in a tokamak plasma with $T_e \sim T_i$, the Z-dependent term in equation (6) is small and $v^2 - \Omega^2 R^2$ is then approximately conserved along the trajectory. In the case of thermalised hypersonically-rotating impurity ions, for which $v^2 \sim T_Z/m_Z$, the presence of the centrifugal potential term in the energy integral prevents individual ions from moving beyond a narrow range of values of R. Hence these ions are deeply trapped.

Wong and Cheng [5] presented numerical calculations of the bounce frequency of centrifugally-trapped impurity ions. We can obtain a simple expression for this frequency using the parallel component of the guiding centre equation of motion, which in the rotating frame can be written in the form [15]

$$m_Z \dot{v}_\parallel = ZeE_\parallel - \mu \nabla_\parallel B_* + \frac{1}{2} m_Z \nabla_\parallel (\Omega^2 R^2), \tag{8}$$

where $v_\parallel$ is the velocity of the guiding centre parallel to the effective magnetic field, $\nabla_\parallel$ denotes the spatial derivative along this direction, and $E_\parallel$ is the parallel component of the electric field given by equation (5). Assuming, as before, that the rotation rate of the frame can be equated to that of the plasma over the particle trajectory (valid for sufficiently narrow orbit widths), the $E_\parallel$ term in equation (8) can be incorporated into the centrifugal force term by defining an effective rotation rate

$$\Omega_* = \Omega \left(1 - \frac{Z m_i T_e}{m_Z (T_i + T_e)} \right)^{1/2} . \tag{9}$$

The other term on the right hand side of equation (8) represents the magnetic mirror force. Given that tokamak magnetic fields vary approximately as $1/R$, it is clear that the equation can be written compactly as

$$\dot{v}_\parallel \simeq \left(v_\perp^2/2 + \Omega_*^2 R^2 \right) \nabla_\parallel (\ln R) . \tag{10}$$

From this form of the equation it is evident that for hypersonically-rotating thermalised minority ions the mirror force will be negligible, and the bounce period will be determined solely by the centrifugal force [modified by the electric field given by equation (5)]. Considering the usual limit of large aspect ratio flux surfaces with circular poloidal cross-section, assuming that particles can undergo only small excursions from the midplane, and writing $v_\parallel = \dot{s}$ where s is the distance of the guiding centre from the midplane along an effective field line, we find that equation (10) then reduces to

$$\ddot{s} = -\frac{\epsilon \Omega_*^2}{q^2} s, \tag{11}$$

where ϵ is the local inverse aspect ratio of the flux surface and q is the effective safety factor, i.e. the number of toroidal circuits made by a field line on the local flux surface in the course of one poloidal circuit. From equation (11) it is immediately apparent that the bounce frequency is $\epsilon^{1/2}\Omega_*/q$ and the bounce period is

$$\tau_b^c = \frac{2\pi q}{\epsilon^{1/2} \Omega_*}. \tag{12}$$

Comparing this result with the bounce period of a magnetically-trapped particle τ_b^m [16], neglecting the Coriolis modification to $\mathbf{B}$, we find that

$$\frac{\tau_b^c}{\tau_b^m} \simeq \frac{v_\perp}{2^{1/2} \Omega_* R}. \tag{13}$$

Hence the centrifugal bounce period will be much shorter than the magnetic bounce period whenever the minority ions are rotating hypersonically. Wong and Cheng [5] solved numerically the guiding centre equations for impurity ions in rotating plasmas, and found a linear correlation between the bounce and rotation frequencies for high values of the latter: this scaling is consistent with the above analysis, and indeed the absolute values of the bounce frequencies obtained by Wong and Cheng are close to those given by our expression for this frequency in the deep centrifugal trapping limit, $\epsilon^{1/2}\Omega_*/q$.

Figure 1 illustrates the phenomenon of centrifugal trapping for the case of a Solov'ev magnetic equilibrium with aspect ratio, shaping and plasma current similar to those of plasmas in the MAST spherical tokamak [9]. The two frames of this figure show the full collisionless orbits of W^{20+} ions initially in the outer midplane with velocity components that are identical except that in the case of the right hand frame the toroidal velocity is boosted by ΩR where $\Omega = 200\,\text{krad s}^{-1}$; toroidal rotation rates of this magnitude have been achieved in MAST through the use of counter-current neutral beam injection [17]. The orbit of this particle was calculated in the laboratory frame using an electric field equal to $-\Omega\nabla\Psi$ plus the expression given by equation (4), with the electron and ion temperatures assumed to be equal. For the orbit shown in the left hand frame, the electric field was taken to be zero. In both cases the particle energy in the plasma rest frame was taken to be 600 eV (a typical mid-radius temperature in MAST). The extreme trapping effect of rotation can be clearly seen; whereas the particle in the left hand plot is free to circulate around the torus poloidally and toroidally, the particle in the right hand plot is prevented by the centrifugal potential well from moving more than a few centimetres from the outer midplane. The bounce period of the orbit shown in the right hand plot is 64.6μs; evaluating the theoretical bounce period given by equation (12), using the appropriate local values of q, ϵ and Ω_*, we obtain 67.1μs. Hence the predicted bounce period lies within 4% of the actual bounce period.

3. Collisional transport

In this section we restrict our attention to the trace impurity limit, which, for a plasma with a single impurity species, requires $n_Z Z^2 \ll n$ where n_Z and n denote the impurity and bulk ion densities [18]. It has been found previously that strong localisation of impurity ions in the outer midplane leads to enhanced neoclassical transport of those ions in the Pfirsch-Schlüter regime [5, 19]. However, as noted by Wong and Cheng [5], impurity ions that are in the Pfirsch-Schlüter regime in a stationary plasma can be in the banana regime in a rapidly rotating plasma, due to their higher bounce frequency. This is important since, for a given collision frequency, transport rates are higher for banana regime particles than they are for those in the Pfirsch-Schlüter regime. In the former case the neoclassical particle diffusivity for a stationary plasma is of the order of the square of the orbit width Δ divided by the product of the collision time τ_c and

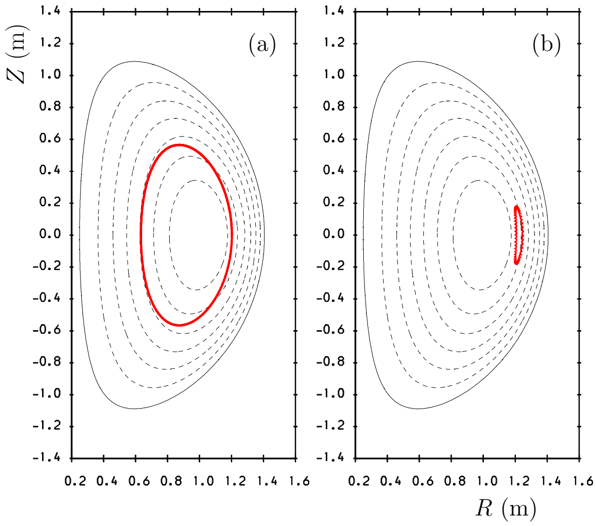

Figure 1: Collisionless orbits of 600 eV W^{20+} ions in (a) non-rotating and (b) transonically co-rotating spherical tokamak plasmas. The ions initially have identical velocity components in the plasma rest frame.

the square root of the local inverse aspect ratio ϵ [16]. This dependence on inverse aspect ratio arises because both the trapped particle fraction and the rate at which particles are detrapped by collisions vary with ϵ. In the case of centrifugal trapping of hypersonically-rotating impurity ions, the trapped particle fraction is essentially unity [5], and the collisional detrapping rate is essentially zero. On the basis of the usual random walk picture of particle transport across magnetic field lines [15], the diffusion rate of banana regime particles would then be expected to be simply Δ^2/τ_c, with no aspect ratio dependence (other than the possible aspect ratio dependence of Δ itself): because of the depth of the centrifugal potential well, a large-angle deflection due to collisions will always transfer a particle into another trapped orbit rather than a circulating one.

Impurity ions of relatively low mass (carbon, for example) are generally in the Pfirsch-Schlüter regime in typical tokamak conditions, even when bulk ions are in the banana regime. The reason for this is apparent from the expression for the collision rate of impurity ions with bulk ions [9]:

$$\frac{1}{\tau_c} = \frac{m_i^{1/2}}{m_Z} \frac{Z^2 e^4 n \ln \Lambda}{6\sqrt{2}\pi^{3/2}\epsilon_0^2 T_i^{3/2}}, \tag{14}$$

where m_i is the bulk ion mass, $\ln\Lambda$ is the Coulomb logarithm and ϵ_0 is the permittivity of free space. Because the mass number of a typical tokamak impurity species is either exactly or approximately equal to twice the atomic number, and tokamak temperatures are generally high enough for such species to be fully ionized, the charge-to-mass ratio is similar to that of the bulk ions, and the collision rate is therefore essentially proportional to Z. The bounce frequency of magnetically-trapped impurity ions, on the other hand, varies inversely as $m_Z^{1/2}$. These two scalings have the effect of making low mass impurity ions much more likely than bulk ions to undergo large angle collisions within a single bounce period, and hence more likely to be in the Pfirsch-Schlüter regime. Several authors have studied the effects of rotation on impurity ion transport in this regime [19, 20, 21], which is generally applicable to low mass impurity ions when the bulk ion flow is subsonic.

The situation is different for a very heavy species such as W in a plasma rotating at a significant fraction of the bulk ion sound speed. In these circumstances the ions are centrifugally trapped, with a bounce frequency that can be much higher than that of magnetically-trapped ions, and does not decrease with the square root of the mass [cf. equation (12)]. Moreover, as commented previously, very massive species are generally only partially ionized under tokamak conditions. In a recent paper Camenen and co-workers [22] assumed a charge state of $Z = 46$ for W ions in tokamak plasmas with temperatures in the range 3-4 keV, while Hinnov and Mattioli [23] estimated $Z \simeq 19 - 34$ for this species in PLT tokamak plasmas, with central electron temperatures of typically around 1 keV. Even lower ionization states would be expected in the relatively cool region close to the plasma edge, where sputtered impurity ions first enter the plasma (although the rotation rate is generally lower here than it is in the plasma centre). It should be noted finally that heavy species such as W have significantly more neutrons than protons, resulting in a further reduction of the charge-to-mass ratio. These considerations suggest that it is possible for very heavy impurity ions in a rotating plasma to be in the banana regime of collisional transport. To quantify this statement, we note from equations (12) and (14) that the ratio of centrifugal bounce time to collision time for an impurity ion is given by

$$\frac{\tau_b^c}{\tau_c} = \frac{m_i^{1/2}}{m_Z} \frac{Z^2 e^4 n \ln \Lambda}{3\sqrt{2}\pi^{1/2}\epsilon_0^2 \epsilon T_i^{3/2}} \frac{q}{\Omega_*}. \tag{15}$$

Evaluating this ratio for a W^{20+} ion in a MAST plasma with $T_i = 600\,\mathrm{eV}$, $n = 3 \times 10^{19}\mathrm{m}^{-3}$, $q = 1$, $\epsilon = 0.3$ and $\Omega_* = 2 \times 10^5\,\mathrm{rad\ s}^{-1}$ we obtain $\tau_b^c/\tau_c \simeq 0.7$. In these circumstances the Pfirsch-Schlüter regime does not apply. It should be noted that this regime may not apply to very massive, partially ionized impurity ions even in the absence of rotation, since the ratio of magnetic bounce period to collision time scales as $Z^2/m_Z^{1/2}$. This ratio has the same dependence on Z as τ_b^c/τ_c, and therefore the condition for impurity ions to be in the Pfirsch-Schlüter regime in a non-rotating plasma and in the banana regime in a rotating plasma does not depend on the impurity ion charge, although it does depend on its mass.

The usual random-walk picture of tokamak transport is simplified in the present case by the fact that the problem is essentially one-dimensional, since the centrifugal potential well restricts the impurity ions to a region (the outer midplane) in which the only significant variations occur in the major radial direction. To estimate the diffusion rate of centrifugally-trapped ions we require an expression for the orbit width, Δ.

As in the case of magnetically-trapped particles, this is determined essentially by the invariance of P_φ in the collisionless limit. The expression for P_φ given by equation (7) differs from the usual expression for toroidal canonical momentum in that it contains an extra term, $m_Z \Omega R^2$. The presence of this extra term, which is associated with the Coriolis force in equation (2), indicates that $m_Z \Omega R^2/Ze$ is effectively added to the poloidal flux. As far as centrifugally-trapped particles are concerned, this means that the poloidal magnetic field is either decreased or increased depending on whether the rotation is in the direction of the plasma current ($\Omega < 0$) or counter to this direction ($\Omega > 0$). The width of the orbit, as in the magnetic trapping case, is essentially equal to the poloidal Larmor radius of the particle [16], but this should be evaluated using the effective poloidal field, taking into account the Coriolis force. The Coriolis modification to the poloidal field can be significant for partially-ionized heavy impurity ions in rapidly rotating plasmas, particularly close to the magnetic axis where, by definition, the poloidal field vanishes in the laboratory frame. Indeed the effective magnetic axis location depends on the rotation rate, as well as the charge and mass of the particles under consideration.

In the limit considered previously of large aspect ratio flux surfaces with circular cross-section, the effective poloidal field is given by

$$B_{*\theta} = \frac{\epsilon B}{q} + \frac{2 m_Z \Omega}{Ze}. \tag{16}$$

Taking the particle diffusivity D_c to be given by the square of the effective poloidal Larmor radius divided by the collision time τ_c and using the expression for τ_c given by equation (14), we obtain for the case of thermalised minority ions

$$D_c \sim \frac{e^2 m_i^{1/2} q^2 n \ln\Lambda}{6\sqrt{2}\pi^{3/2}\epsilon_0^2 \epsilon^2 B^2 T_i^{1/2}} \left[1 + 2\frac{q}{\epsilon}\frac{\Omega}{\omega_Z}\right]^{-2}, \tag{17}$$

where $\omega_Z = ZeB/m_Z$ is the minority ion cyclotron frequency. It is important to note that whereas the leading order term on the right hand side is independent of Ω, Z and m_Z, the Coriolis correction term depends on all of these parameters and moreover changes sign when the sense of rotation is changed from co-current ($\Omega < 0$) to counter-current ($\Omega > 0$). Equation (17) indicates that centrifugally-trapped impurity ions are more rapidly transported by collisions in co-rotating plasmas than they are in counter-rotating plasmas. There is a straightforward physical reason for this. In the rest frame of a co-rotating plasma, the effective poloidal magnetic field in the outer midplane is reduced, causing an increase in the drift orbit excursions of impurity ions, which are consequently transported across the plasma more rapidly than they would in the absence of the Coriolis force. In a counter-rotating plasma, the effective poloidal field in increased, thereby suppressing transport.

The leading order term in equation (17) differs from the banana regime diffusivity in a non-rotating plasma by an extra factor of order $1/\epsilon^{1/2}$ [16]. However, as discussed earlier the relevant comparison here is with the Pfirsch-Schlüter diffusivity D_{PS}, since impurity ions in non-rotating tokamaks tend to be in this regime. A simple random-walk estimate gives $D_{PS} \sim q^2\rho^2/\tau_c$, where ρ is the ion Larmor radius [15]. Combining this expression with equation (17), and neglecting the Coriolis correction term in the latter, we obtain

$$D_c \sim D_{PS}/\epsilon^2. \tag{18}$$

We infer from this that centrifugal trapping is likely to produce a significant enhancement in neoclassical transport, particularly in the core region of conventional tokamaks where $\epsilon \ll 1$. Using test-particle simulations of impurity ion guiding centre orbits in TFTR, Wong and Cheng [5] computed diffusion rates in rapidly rotating plasmas exceeding those in stationary plasmas by a factor that increased towards the magnetic axis and, except very close to the axis, was of the order of $1/\epsilon^2$, broadly consistent with equation (18) (cf. figure 9 in Ref [5]).

We now consider the advective transport of massive impurity ions that are confined to the outer midplane. Steady-state momentum balance for the impurity ion fluid in a frame co-rotating with the bulk ions can be described approximately by the equation

$$Ze\mathbf{v}\times\mathbf{B}_* + \frac{1}{2}m_Z\Omega_*^2\nabla(R^2) - \frac{m_z}{\tau_c}\mathbf{v} = \mathbf{0}, \tag{19}$$

where we have included a drag term, representing the collisional interaction of impurity ions with bulk ions. The pressure gradient term in the momentum balance equation can be neglected when, as in the present case, the impurity ions are assumed to be rotating hypersonically with respect to their own thermal velocity. Because it is confined to the outer midplane [cf. equation (1)], the impurity ion fluid has zero net poloidal flow, and the major radial component of equation (19) thus reduces to

$$Zev_\varphi B_{*\theta} + m_Z\Omega_*^2 R - \frac{m_Z v_R}{\tau_c} = 0. \tag{20}$$

Hence in steady-state the impurity ions have a net toroidal flow in the rotating frame given by

$$v_\varphi = -\frac{m_Z\Omega_*^2 R}{ZeB_{*\theta}} + \frac{m_Z v_R}{Ze\tau_c B_{*\theta}}. \tag{21}$$

Using equations (14) and (16), assuming that the effective poloidal cyclotron frequency of the impurity ions is large compared to their collision frequency, we find that the toroidal component of equation (19) then yields the following radial drift velocity in the large aspect ratio, circular cross-section limit:

$$v_R \equiv v_c \simeq \frac{e^2 m_i^{1/2} m_Z q^2 \Omega_*^2 R n \ln\Lambda}{6\sqrt{2}\pi^{3/2}\epsilon_0^2\epsilon^2 B^2 T_i^{3/2}}\left[1 + 2\frac{q}{\epsilon}\frac{\Omega}{\omega_Z}\right]^{-2}. \tag{22}$$

Examination of equations (21) and (22) indicates that the $m_Z(\mathbf{v}\cdot\nabla)\mathbf{v}$ term in the rotating frame impurity ion momentum balance equation can be neglected provided that the effective rotation frequency is small compared to the effective impurity ion poloidal cyclotron frequency. Whereas the leading order term in D_c is independent of both the charge and mass of the impurity ions, the leading order term in v_c is proportional to m_Z, and therefore the advective transport described by equation (22) is likely to be most important for very heavy impurities such as tungsten. It is also important to observe that v_R is positive, i.e. it represents an outward advection of particles. We note finally that the calculation of v_c, unlike that of D_c, does not require any assumptions to be made regarding the ordering of τ_b^c/τ_c and therefore applies equally to the banana and Pfirsch-Schlüter regimes. Equations (17) and (22) indicate that

$$\frac{v_c}{D_c} \sim \frac{m_Z R\Omega_*^2}{T_i} = \frac{M_{*Z}^2}{R}, \tag{23}$$

where $M_{*Z} = R\Omega_*(m_Z/T_i)^{1/2}$ is the effective impurity ion Mach number. Assuming that the impurity ion density length scale is of the order of the plasma minor radius a, we infer from equation (23) that the ratio of advective particle flux ($v_c n_Z$) to diffusive flux ($D_c \nabla n_Z$) is of order $\epsilon_a M_{*Z}^2$ where $\epsilon_a = a/R$. The density scale length could of course be significantly smaller than a, for example in the vicinity of an internal transport barrier, in which case the predicted ratio of advective to diffusive flux would be smaller.

In the above calculation of v_c we neglected the presence of a toroidal electric field E_φ associated with the plasma loop voltage, which leads to an inward pinch of trapped particles, the pinch velocity v_p being $-E_\varphi/B_\theta$ [24]. This effect, which counteracts the outward advection described above, will also be modified by the Coriolis force; using equation (16) we find that the pinch velocity is given by

$$v_p \simeq -\frac{qE_\varphi}{\epsilon B}\left[1 + 2\frac{q}{\epsilon}\frac{\Omega}{\omega_Z}\right]^{-1}. \tag{24}$$

As in the case of the diffusivity and the outward advection given by equation (22), the Coriolis correction to v_p depends on the sign of the rotation, with a higher pinch velocity predicted in the presence of co-rotation ($\Omega < 0$). Very close to the magnetic axis, however, v_p changes sign in the co-rotating case and augments v_c rather than opposing it.

It should be noted that the expressions given by equations (17), (22) and (24) remain well-behaved when $\epsilon \to 0$. In this limit the effective poloidal field is dominated by the Coriolis term in equation (3), and it is this term that then determines both the diffusive and advective contributions to the particle flux in the banana regime. However, the expressions cease to be valid if $B_{*\theta} \to 0$ for $\epsilon \neq 0$, which occurs in the case of co-rotation. In the immediate vicinity of the effective magnetic axis the assumption of narrow orbit widths does not apply, and the orbits are potato-like rather than banana-like [16].

4. Test-particle simulations

In order to quantify the effects on global particle confinement of the effects discussed in the previous section we return to the MAST-like equilibrium used to generate the orbits in figure 1. Specifically, we use an orbit-following code `CUEBIT` [9] to calculate the orbits of 10^4 tungsten ions initially at the magnetic axis, taking collisions with rotating bulk ions into account. Tungsten is not a naturally-occurring impurity species in MAST; we have chosen this species and this device in order to illustrate the extreme consequences for collisional impurity transport of a combination of high impurity mass, moderate impurity charge, high plasma rotation and low magnetic field. `CUEBIT` is used to track impurity ion orbits in the laboratory frame by solving the equation [9]

$$m_Z \frac{d\mathbf{v}}{dt} = Ze(\mathbf{E}_i + \mathbf{v} \times \mathbf{B}) - \frac{m_Z}{\tau_c}(\mathbf{v} - R\Omega_\varphi \mathbf{e}_\varphi) + m_Z \mathbf{r}(t). \tag{25}$$

Here $\mathbf{e}_\varphi$ is the unit vector in the toroidal direction and $\mathbf{r} = (r_x, r_y, r_z)$ is a set of random numbers, chosen independently for each particle and at each time step, with zero mean and variance

$$\sigma^2 = \frac{u_i^2}{\tau_c \Delta t}, \tag{26}$$

$u_i = (2T_i/m_Z)^{1/2}$ being the desired test particle thermal speed and Δt the time step used in the code. The drag term in equation (25) ensures that the impurity ions acquire a mean toroidal flow close to that of the bulk ions, and the random (Langevin) term ensures that the impurity ion velocity distribution relaxes to a drifting Maxwellian with the local bulk ion temperature. The algorithm used in `CUEBIT` guarantees conservation of kinetic energy to machine accuracy in the absence of electric fields and collisions [25]. The time taken for the number of ions in the system to drop to $1/e$ of its initial value gives us a measure of the global neoclassical confinement time. For the purpose of modelling collisions with bulk ions, the background temperature and density were assumed to be linear functions of Ψ, with T_i ranging from 0.1 keV at the edge to 1 keV in the core and n ranging from 10^{19}m^{-3} to $5 \times 10^{19}\text{m}^{-3}$. In the presence of rotation the density of bulk ions is not a flux function [14], although the inboard/outboard asymmetry is much less extreme than it is for massive impurity species, and for simplicity we neglect it here, along with the small modifications to Solov'ev equilibria arising from rotation [26]. We model the Ware pinch by assigning a finite, uniform value to E_φ (0.3Vm^{-1}).

Table 1 lists the computed confinement times in ms of W^{10+}, W^{15+} and W^{20+} ions in stationary, counter-rotating and co-rotating plasmas (in the latter two cases the entire plasma is assumed to rotate as a single rigid body). For non-rotating plasmas, there is a modest monotonic rise in the confinement time with increasing Z. This may reflect the fact that impurity ions of a given mass become progressively more collisional, and are therefore transported at the relatively slow Pfirsch-Schlüter rate over a greater region of the plasma, as Z is increased. In the trace impurity limit that we are considering, the impurity ions make a negligible contribution to the total ion current, and therefore the neoclassical theory prediction of impurity ion density peaking at the magnetic axis, required by ambipolarity [16], does not apply to these simulations.

Table 1: Confinement times in ms of W ions in stationary and rotating MAST-like plasmas

Z	Stationary	Counter-rotating	Co-rotating
10	232.6	8.1	0.8
15	267.6	6.3	1.4
20	298.4	5.6	2.1

The most striking feature of the results in Table 1 is a sharp drop in the confinement time, from several hundred ms to a few ms or less, when the plasma is either co-rotating or counter-rotating. Indeed the computed confinement times in the rotating cases are significantly lower than typical H-mode energy confinement times in MAST ($\sim 20-50\,\mathrm{ms}$), which are determined by turbulent rather than neoclassical transport [17]. There is also a clear co/counter asymmetry, which diminishes with increasing Z, with more rapid transport occurring in the co-rotating case.

A quantitative analysis of impurity ion transport in these simulations can be carried out by computing moments of the spatial distribution of impurity ions. For the case of impurity ions in a plasma counter-rotating at 2×10^5rad s^{-1} we computed $\langle\delta R\rangle = \langle(R-R_i)\rangle$, the mean deviation in major radius of the ions from their initial position R_i, and $\langle\delta R\rangle^2 = \langle(R-R_i-\delta R)^2\rangle$, the mean squared deviation. For these particular simulations 10^3 particles were used, initially in the midplane with R_i midway between the magnetic axis and the plasma edge, and with a Maxwellian velocity distribution at the local bulk ion temperature, drifting toroidally at the local bulk ion toroidal velocity. For sufficiently short times after $t=0$ we can assume that the transport coefficients are those corresponding to $R=R_i$, $Z=0$, and, given the fact that collisional transport essentially occurs in the R direction only in the circumstances under consideration (i.e. deep centrifugal trapping), we can model the transport using a simple diffusion-advection equation of the form

$$\frac{\partial n_Z}{\partial t} + v_R\frac{\partial n_Z}{\partial R} = D_R\frac{\partial^2 n_Z}{\partial R^2}, \tag{27}$$

where D_R and v_R are the diffusivity and advection velocity (the advection is outward if $v_R>0$). For the case of N particles lying initially at $R=R_i$, neglecting losses (i.e. assuming that R is effectively unbounded), equation (27) has solution

$$n_Z = \frac{N}{(\pi D_R t)^{1/2}}\exp\left[-\frac{(R-v_Rt-R_i)^2}{4D_Rt}\right]. \tag{28}$$

It is straightforward to show from this result that

$$\langle\delta R\rangle = v_R t, \tag{29}$$

and

$$\langle \delta R^2 \rangle = 2D_R t. \tag{30}$$

The solid squares in figure 2 show $\langle \delta R \rangle$ as a function of time for W^{20+} ions. It is clear from this figure that, except for the first 300μs or so (around two collision times), $\langle \delta R \rangle$ varies linearly with time. The corresponding advection velocity, i.e. the gradient of the linear portion of this curve, is approximately $50\,\mathrm{ms}^{-1}$. Substituting appropriate local values of parameters into equations (22) and (24) we obtain $v_c + v_p \simeq 63\,\mathrm{ms}^{-1}$ (in this case v_c exceeds $|v_p|$ by a factor of around 20). We conclude that the advection velocity observed in the simulation is broadly consistent with theoretical predictions based on the assumptions of deep centrifugal trapping and large aspect ratio, circular flux surfaces. For the particular scenarios considered in the simulations we find in general that $v_c \gg |v_p|$, i.e. the Ware pinch does not contribute significantly to the advective component of the particle flux, which is consequently directed outward.

In order to check the predicted scaling of v_c with m_Z a second simulation was carried out with parameters that were identical except that both A and Z were reduced by a factor of 2, i.e. the impurity ions were assumed to be Mo^{10+} (molybdenum-92). By reducing A and Z by the same factor we ensure that ω_Z is unchanged, and therefore the predicted v_c is reduced while v_p remains constant. The mean radial excursion of these ions is shown as a function of time by the open squares in figure 2. It is apparent that the net advection velocity has been reduced by slightly more than a factor of 2, consistent with equations (22) and (24) in the limit $v_c \gg |v_p|$.

Figure 3 shows $\langle \delta R \rangle^2$ versus time in the W^{20+} and Mo^{10+} simulations. The results are somewhat less clear-cut than those in figure 2, but we again observe an approximately linear variation after an initial transient phase lasting for a period of the order of the collision time. The diffusion rates inferred from the linear parts of these curves are of the order of the predicted rate given by equation (17), but there is some evidence in the figure of a dependence of D_c on m_Z and/or Z that is not consistent with the theoretical prediction, with the molybdenum ions having a somewhat higher diffusivity. This may be due to the fact that the molybdenum ions are less collisional than the tungsten ions, and therefore the approximations used to obtain equation (17) are satisfied to a greater extent in the former case. However in both cases we find that $\epsilon_a M_{*Z}^2 \gg 1$, and therefore the transport is dominated by outward advection. This is reflected by the fact that the advection velocity corresponding to the slope of the W^{20+} curve in figure 2 implies a confinement time of a few ms, which is consistent with the value given in Table 1 (5.6 ms).

The differences in confinement times between stationary and rotating plasmas indicated in Table 1 are consistent with the conjecture that transport in the rotating cases is essentially advective, with an advection velocity given approximately by equation (22). The co/counter asymmetry in the confinement times, and the dependence of this asymmetry on Z, is also consistent with the analysis in the previous section: for ions of a given mass in plasmas rotating at a given absolute rate, the predicted Coriolis

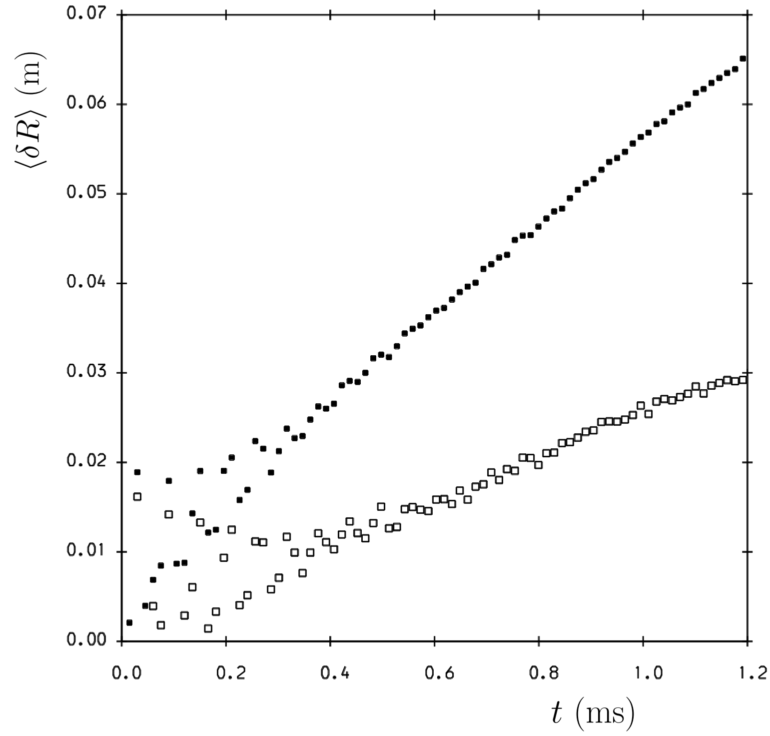

Figure 2: Mean excursion in major radius of impurity ions with $A = 184$, $Z = 20$ (solid squares) and $A = 92$, $Z = 10$ (open squares). In both cases the impurity ions were launched in the outer midplane, midway between the magnetic axis and the plasma edge, with a mean flow velocity equal to the local bulk ion toroidal rotation velocity.

modification to the transport coefficients is inversely proportional to the ion charge. For tungsten ions with $Z = 10 - 20$ we find that $2q\Omega/(\epsilon\omega_Z)$ can be of order unity or more over a significant fraction of the plasma volume: this accounts for the very large differences between the confinement times for co-rotating and counter-rotating plasmas listed in Table 1, particularly in the case of $Z = 10$. In the case of co-rotation, as noted previously, the two terms in our expression for the effective poloidal magnetic field [equation (16)] are of opposite sign, and $B_{*\theta}$ vanishes for finite ϵ. Although the approximations used to obtain expressions for D_c and v_c break down under these circumstances, we would nevertheless expect rapid collisional transport to occur.

Insight into the role played by the Coriolis force in these simulations can be gained by plotting effective flux surfaces in the rotating frame for W ions, taking into account the $m_Z\Omega R^2/Ze$ contribution to Ψ. Figure 4 shows the effective flux contours for the three rotation scenarios we have considered and $Z = 20$. The actual plasma boundary is shown as a solid contour in each case. It is clear from these plots that counter-rotation effectively compresses the flux surfaces whereas co-rotation causes them to expand beyond the plasma boundary, with a pronounced outward shift in the magnetic axis. In these circumstances it is not surprising that W ions are more rapidly ejected from

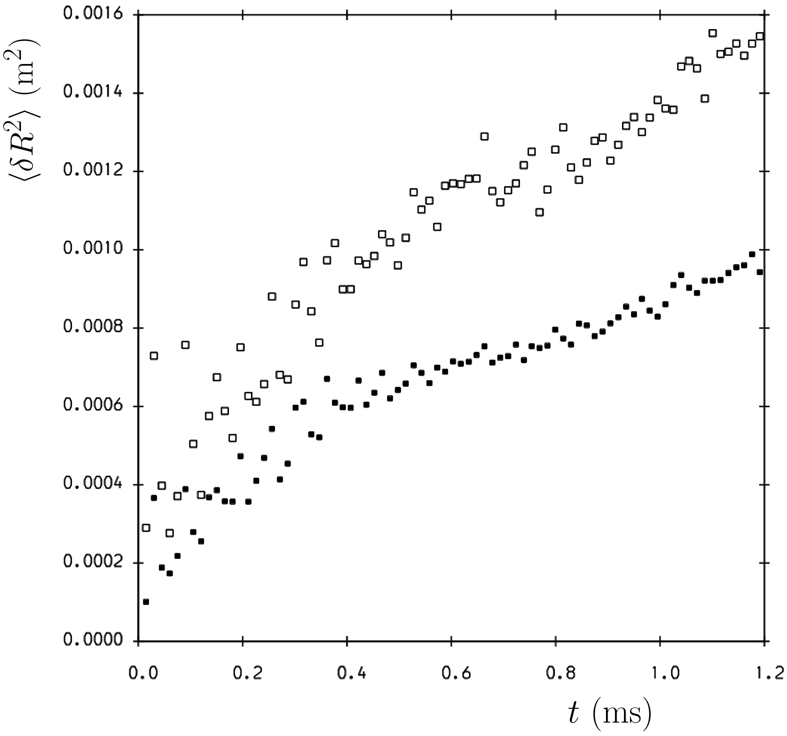

Figure 3: Mean squared deviation from average major radius of impurity ions with $A = 184$, $Z = 20$ (solid squares) and $A = 92$, $Z = 10$ (open squares).

a co-rotating plasma than they are from a counter-rotating one.

Figure 5 shows snapshots of the distributions of W^{10+} ions in the poloidal plane in the simulations with $\Omega = 0$ ($t = 250\,\mathrm{ms}$) and $\Omega = 2 \times 10^5\,\mathrm{rad\ s^{-1}}$ ($t = 10\,\mathrm{ms}$). These snapshots were taken at times slightly longer than the particle confinement times in each case. When ions cross the plasma boundary the code stops tracking the orbit, and the recorded position in figure 5 is thus the point at which the ion leaves the plasma. In the non-rotating case the ions are distributed across the plasma cross-section, although there is a slight up-down asymmetry in the losses, reflecting the direction of the grad-B and curvature drifts. In the rotating case, as expected from the analysis in section 2, the ions all lie close to the outer midplane and, unlike the non-rotating case, no ions remain close to the magnetic axis. This last observation is further clear evidence that the collisional transport of hypersonically-rotating massive ions is essentially advective.

Simulations were also performed for fully-ionized tungsten ($Z = 74$). The confinement times were again found to be very short, and almost identical for counter-rotating and co-rotating plasmas (5.8 ms and 5.2 ms respectively). In this case we would expect the Pfirsch-Schlüter regime to apply; the short confinement times are attributable to the fact that the rapid outward advection described by equation (22) is applicable to all collisionality regimes, and the absence of significant co/counter asymmetry is

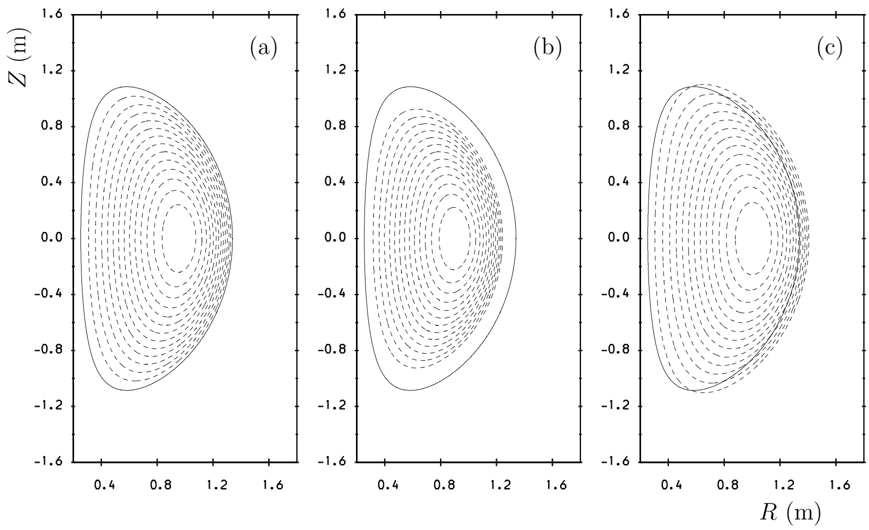

Figure 4: Effective flux surfaces for W^{20+} ions in (a) stationary, (b) counter-rotating and (c) co-rotating MAST-like plasmas. In (b) and (c) the absolute value of the rotation rate is 2×10^5 rad s^{-1}. The plasma boundary is shown as a solid contour in all three cases.

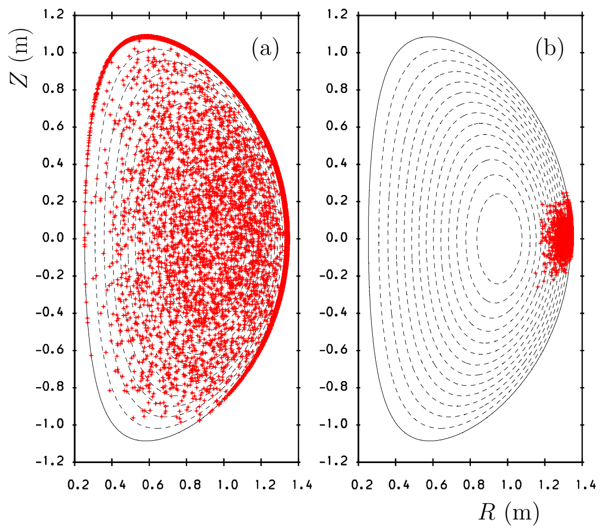

Figure 5: Distribution of W^{10+} ions in the (R, Z) plane for (a) $\Omega = 0$, $t = 250\,$ms and (b) $\Omega = 2 \times 10^5$ rad s^{-1}, $t = 10\,$ms.

attributable to the fact that the rotation parameter $2q\Omega/(\epsilon\omega_Z)$ is very small over almost the entire plasma volume.

5. Conclusions and discussion

In this paper we have considered the orbital dynamics and collisional transport of heavy trace impurity ions in toroidally-rotating tokamak plasmas. It has been known for some time that under equilibrium conditions such ions are concentrated on the low field side of the plasma, due to the net effect of the centrifugal force and an electric field required to maintain quasineutrality [8]. We have pointed out that this poloidal localisation requires that individual ions are deeply trapped, by a centrifugal potential well rather than a converging magnetic field, and shown that the bounce frequency can be much higher than that of magnetically-trapped ions, and higher than the collision rate. As first noted by Wong and Cheng [5], the commonly-held assumption that heavy impurity ions are generally in the highly collisional (Pfirsch-Schlüter) regime of neoclassical transport thus requires re-examination in the presence of toroidal rotation. We have also considered the modification to the effective magnetic field arising from the Coriolis force. Taking these effects into account, we have obtained simple expressions for the diffusivity and advection velocity of heavy trace impurity ions. These expressions indicate that centrifugal trapping increases the particle diffusivity above the conventional Pfirsch-Schlüter value by a factor of order $1/\epsilon^2$ where ϵ is the local inverse aspect ratio. Moreover, irrespective of the collisionality regime, the interaction of centrifugally-trapped massive impurity ions with bulk ions leads to an outward advection that is proportional to the impurity ion mass and, for heavy species such as tungsten, can exceed the pinch velocity associated with the loop voltage. Due to the presence of the Coriolis force, heavy trace impurity ions are transported at a higher rate in plasmas rotating in the plasma current direction than they are in plasmas rotating counter to the plasma current.

With regard to this last point, it should be noted that the orbits of bulk ions will also be altered by the Coriolis modification to the effective field, and it may be expected that this modification will affect to some extent the transport of those ions. For electrons, on the other hand, the rotation rates that can be achieved in tokamak plasmas are sufficiently low that both the centrifugal and Coriolis forces are completely negligible.

We have illustrated the effects of toroidal rotation on heavy trace impurity transport using test-particle simulations of tungsten and molybdenum ion orbits in transonically-rotating spherical tokamak plasmas. In these simulations it is found that rotation reduces the confinement time of W ions by around two orders of magnitude, with significant differences between co-current and counter-current rotation that are consistent with analytical predictions based on Coriolis force modifications to the effective magnetic field. It is worth noting in this context that Camenen and co-workers [22] have recently found that the Coriolis force can also have a significant effect on the turbulent transport of impurity ions, particularly those with low Z/A. Computing the spatial moments of the impurity ion distributions in our simulations, we have found that the reduction in confinement observed in the presence of rotation can be attributed mainly to advection rather than diffusion.

Any comparison between collisional transport calculations and experimental data for rotating plasmas is complicated by the fact that turbulent transport tends to be suppressed to some extent in the presence of rotation shear, and moreover the properties of counter-rotating plasmas are generally very different from those of co-rotating plasmas with similar momentum sources in the same device, not least because of higher impurity sputtering rates due to beam ion losses in the counter-rotating case [17]. These caveats notwithstanding, it is notable that several independent experimental studies in limiter tokamaks consistently indicated higher confinement of impurities, including tungsten, with counter-current beam injection (hence counter-rotation) than with co-current injection [6, 7, 27, 28, 29]. A possible explanation of this result was provided by Burrell and co-workers [20], who considered the Pfirsch-Schlüter regime transport of impurity ions with thermal velocities comparable to the plasma rotation velocity, and found a greater inward flux of impurities for counter-rotation than co-rotation, assuming fixed absolute momentum input and plasma profiles. In the case of the TFTR experiments Wong and Cheng [5] showed that it was possible for the impurity ions to be in the banana regime in the presence of high rotation. In an earlier analysis, Wong [10] found a rotation-induced enhancement in the neoclassical transport of impurities in the banana regime, but could not account for the observed co/counter asymmetry. Both our results and those of Wong and Cheng [5] are consistent with the limiter tokamak data insofar as they indicate that retention of heavy impurity ions in rotating plasmas is greater if the sense of rotation is counter to the plasma current, although we stress that the advection described by equation (22) is always outward, irrespective of the sign of Ω.

In recent years toroidal rotation velocities close to or (in the case of MAST) exceeding the bulk ion thermal speed have been achieved in several divertor tokamaks, including JET [30]. When tungsten is introduced into the first wall of JET, it may be expected that ions of this species will be present, and that in rapidly-rotating plasmas they will have toroidal velocities far in excess of their own thermal speed, giving rise to centrifugal trapping. Our analysis suggests that W ions in JET could then undergo rapid collisional transport, depending on the local values of rotation velocity and ion temperature. As noted previously, the first wall of Asdex Upgrade already incorporates tungsten [4]: a systematic study of W transport specifically in rapidly-rotating plasmas in this device would be of considerable interest. In the case of ITER relatively low rotation rates are expected: calculations by Staebler and St John [31] indicate rotation velocities of about 160 km s^{-1} in the core of a baseline scenario ITER plasma, where $T_i \simeq T_e \simeq 20\,\mathrm{keV}$, $n \simeq 10^{20}\,\mathrm{m}^{-3}$, $q \simeq 1$. For these parameters the predicted advection velocity v_c would be very small. Tungsten ions would be fully-stripped and supersonic, but their collision time ($\simeq 60\,\mu$s) would be substantially shorter than their centrifugal bounce period ($\sim 600\,\mu$s), and therefore they would not be in the centrifugal banana regime. Our results may nevertheless have relevance for other proposed experiments, in particular CTF [2]; modelling of momentum sources and transport in this proposed device indicate toroidal Mach numbers close to unity [32].

We comment finally that all of the analytical results obtained in this paper could, of course, have been obtained by considering impurity ion orbits in the laboratory frame, without considering explicitly the effects of the centrifugal and Coriolis forces. Indeed, the numerical results discussed in section 4 were obtained by solving the Lorentz force equation in an inertial frame. In this frame impurity ion trapping can be attributed to an electrostatic force rather than a centrifugal one. However, the dynamical behaviour of the impurity ions can be more clearly understood if one considers their orbits in the rotating frame.

Acknowledgments

Helpful conversations with A Thyagaraja are gratefully acknowledged. We are also grateful to the referees, whose comments led to significant improvements in the paper. This work was supported by the United Kingdom Science & Technology Facilities Council (through a CASE studentship), the United Kingdom Engineering and Physical Sciences Research Council, and the European Communities (under the Contract of Association between EURATOM and UKAEA). The views and opinions expressed herein do not necessarily reflect those of the European Commission.

References

[1] Aymar R, Barabaschi P and Shimomura (for the ITER Team) 2002 *Plasma Phys. Control. Fusion* **44** 519

[2] Morris A W, Akers R J, Counsell G F, Hender T C, Lloyd B, Sykes A, Voss G M and Wilson H R 2005 *Fusion Eng. and Des.* **74** 67

[3] Hirai T, Linke J, Rubel M, Coad J P, Likonen J, Lungu C P, Matthews G F, Philipps V and Wessel E 2008 *Fusion Eng. Des.* **83** 1072

[4] Neu R, Dux R, Kallenbach A, Pütterich P, Balden M, Fuchs J C, Herrmann A, Maggi C F, OMullane M, Pugno R, Radivojevic I, Rohde V, Sips A C C, Suttrop W, Whiteford A and the ASDEX Upgrade Team 2005 *Nucl. Fusion* **45** 209

[5] Wong K L and Cheng C Z 1989 *Phys. Fluids B* **1** 545

[6] Suckewer S, Cavallo A, Cohen S, Daughney C, Denne B, Hinnov E, Hosea J, Hulse R, Hwang D, Schilling G, Stratton B and Wilson R 1984 *Nucl. Fusion* **24** 815

[7] Wong K L, Cheng C Z, Stratton B and Ramsey A 1987 *14th. Eur. Conf. on Controlled Fusion and Plasma Physics (Madrid, Spain)* (Brussels: European Physical Society) p 121

[8] Wesson J A 1997 *Nucl. Fusion* **37** 577

[9] McKay R J, McClements K G, Thyagaraja A, Fletcher L 2008 *Plasma Phys. Control. Fusion* **50** 065017

[10] Wong S K 1987 *Phys. Fluids* **30** 818

[11] Jackson J D 1975 *Classical Electrodynamics* 2nd Edn (New York: Wiley) p 574

[12] Thyagaraja A and McClements K G 2009 UKAEA report UKAEA FUS 555 (available at http://www.fusion.org.uk/techdocs/index.htm)

[13] Thyagaraja A and McClements K G 2006 *Phys. Plasmas* **13** 062502

[14] Hinton F L and Wong S K 1985 *Phys. Fluids* **28** 3082

[15] Helander P and Sigmar D J 2002 *Collisional Transport in Magnetized Plasmas* (Cambridge: Cambridge University Press)

[16] Wesson J A 2003 *Tokamaks* 3rd Edn (Oxford: Clarendon Press)

[17] Akers R J *et al* 2005 *Proc. 20th IAEA Fusion Energy Conference* (Vilamoura, Portugal, 2004) paper EX/4-4 (Vienna: IAEA)

[18] Burrell K H and Wong S K 1981 *Phys. Fluids* **24** 284

[19] Romanelli M and Ottaviani M 1998 *Plasma Phys. Control. Fusion* **40** 1767

[20] Burrell K H, Ohkawa T and Wong S K 1981 *Phys. Rev. Lett.* **47** 511

[21] Fülöp T and Helander P 1999 *Phys. Plasmas* **6** 3066

[22] Camenen Y, Peeters A G, Angioni C, Casson F J, Hornsby W A, Snodin A P and Strintzi D 2009 *Phys. Plasmas* **16** 012503

[23] Hinnov E and Mattioli M 1978 *Phys. Lett.* **A66** 109

[24] Ware A A 1970 *Phys. Rev. Lett.* **25** 15

[25] Hamilton B, McClements K G, Fletcher L and Thyagaraja A 2003 *Solar. Phys.* **214** 339

[26] Savenko N, McClements K G and Thyagaraja A 2006 *33rd EPS Conf. on Plasma Physics (Rome, Italy)* ECA Vol. 30I P-1.094

[27] Lyon J F, Isler R C, Murakami M, Bush C E, Dunlap J L, Howe H C, Jahns G L, Ketterer H E, Mihalczo J T, Neidigh R V, Paré V K and Wolgen J B 1977 *8th European Conference on Controlled Fusion and Plasma Physics (Prague, Czechoslovakia)* (Prague: Czechoslovak Academy of Sciences) Vol 1, p 23

[28] Suckewer S *et al.* 1981 *Nucl. Fusion* **21** 981

[29] Isler R C, Murray L E, Crume E C, Bush C E, Dunlap J L, Edmonds P H, Kasai S, Lazarus E A, Murakami M, Neilson G H, Pare V K, Scott S D, Thomas C E and Wootton A J 1983 *Nucl. Fusion* **23** 1017

[30] de Vries P C, Hua M-D, McDonald D C, Giroud C, Janvier M, Johnson M F, Tala T, Zastrow K-D and JET EFDA Contributors 2008 *Nucl. Fusion* **48** 065006

[31] Staebler G M and St John H E 2006 *Nucl. Fusion* **46** L6

[32] Cottrell G A and Kemp R 2009 *Nucl. Fusion* **49** 042001